One-step solution combustion synthesis of $K_{0.5}Na_{0.5}NbO_3$ powders at a large-scale

Nan Sheng [a], Cheng-gong Han, Chunyu Zhu [a] *, Tomohiro Akiyama

[a] Faculty of Engineering, Hokkaido University, Sapporo 060-8628, Japan

*Corresponding author: Tel.: +81-11-706-6842

E-mail address: chunyu6zhu@eng.hokudai.ac.jp (Chunyu Zhu)

Abstract

In this work, fine powders of $K_{0.5}Na_{0.5}NbO_3$ (KNN) are produced by a single step of solution combustion synthesis (SCS) using glycine as the reductant fuel and potassium & sodium nitrates as the oxidizers, which are mixed with niobium oxide. Single phase of KNN products can be successfully prepared in a one-step SCS by adjusting the glycine-nitrate ratio. It is concluded that the stoichiometric or slightly fuel-excess condition is good for the single step production of KNN. The one-step SCS of KNN also shows good scaling-up productivity, which can be ignited by both electric heating and microwave heating. This work may provide a feasible large-scale production of various functional oxides by a one-step SCS process.

Keywords: solution combustion synthesis, oxide, KNN, piezoelectric, ceramic powder

1. Introduction

The preparation of inorganic oxide fine powders has attracted significant attentions in recent years. Inorganic fine powders are of interest in ceramics for structural applications and new insights into their functional properties such as magnetic, electric, or optical characteristics. [1, 2] The piezoelectric ceramics, such as $Pb(Zr,Ti)O_3$ and $Pb(Mg_{1/3},Nb_{2/3})O_3$, have numerous applications such as sensors, actuators, and transduces. Lead-free potassium-sodium-niobates ($K_xNa_{1-x}NbO_3$) have been extensively studied for replacing $Pb(Zr,Ti)O_3$-based ceramics because of environmental issues. Among them, the perovskite-type $K_{0.5}Na_{0.5}NbO_3$ (KNN) has been the most investigated candidate because it has a high Curie temperature, a high electromechanical coupling coefficient and a relatively low dielectric constant. [3-6]

The alkaline niobate ceramics are very difficult to be synthesized by conventional solid-state reaction because the high-temperature sintering often leads to stoichiometric deviation in the composition of the final product. [7, 8] Several methods have been employed for the synthesis of KNN, such as the direct sintering of ammonium niobium oxalate and $C_4H_4O_6KNa \cdot 4H_2O$, [9] hydrothermal synthesis, [10] citrate precursor technique, [11] and combustion synthesis. [12-14] Solution combustion synthesis (SCS) of ceramic powders have attracted much more attentions because of its advantages over the others, such as high degree of chemical homogeneity, a single step for the synthesis of ceramic powders, and elimination of

ball-milling procedures.[15-20] SCS is a combustion synthesis process based on a highly exothermic, self-sustaining reaction, which is generated by heating a mixture of aqueous metal nitrates and hydrocarbon fuels such as urea and glycine. This approach has been applied for the preparation of a variety of functional oxides. [21-27] The preparation of KNN by combustion synthesis have been reported by several groups, for example, Yang et al. reported the direct synthesis of KNN powders using Na_2CO_3, K_2CO_3 and Nb_2O_5 as raw materials and urea as fuel, which were calcined at 500~700 ºC; [13] a similar preparation process was also reported by Kumar et al., using urea as the fuel. [28] However, these processes are not the self-sustaining one, which cannot produce KNN in a fast one-step synthesis.

Here, we report the synthesis of KNN using a one-step glycine-nitrate SCS process, in which glycine is used as the reductant fuel, while potassium and sodium nitrates are used as the oxidizers. The raw materials are mixed with niobium oxide to produce KNN directly. The effect of glycine ratio on the product purity and the scalability of the SCS process are studied in details.

2. Experimental section

Material preparation: All reagents used in this study were commercially available and used as

supplied without further purification: potassium nitrate (KNO_3, 99.9%, Kishida Chemical Co., Ltd., Japan), sodium nitrate ($NaNO_3$, 99.9%, Kishida Chemical Co., Ltd., Japan), glycine (H_2NCH_2COOH, > 99%, Kishida Chemical Co., Ltd., Japan), and niobium oxide (Nb_2O_5, 99.9%, High Purity Chemicals).

Figure 1 shows the schematic diagram of the SCS of KNN, which is modified from previous studies. [23, 24, 29, 30] In a typical synthesis required for preparing 3 g of KNN, potassium nitrate, sodium nitrate and niobium oxide were weighed in a molar ratio of K:Na:Nb = 0.5:0.5:1, which were dissolved/mixed in distilled water in an alumina crucible. It is noted that niobium oxide was in a powder form, which did not dissolve in water. The suspension solutions were subsequently mixed with different amount glycine fuel (to make different combustion equivalence ratio, ϕ) and stirred. The as-prepared suspension solutions were further heated on a hot plate while being stirred to evaporate excess water until dried gels were formed. The dried gel in the crucible was transferred to a lab-made combustion synthesis apparatus, as shown in Figure 1. The reactor consisted of a stainless-steel bin with a long vertical stainless-steel mesh chimney, which enabled the safe removal of large amounts of gases during combustion, leaving behind the ash reactant remnants in the reactor to be collected after the reaction. The reactor was placed in an electric mantle heater, which was pre-heated to and maintained at 400 ºC. The gel mixtures self-ignited under heating along with the emission of

gases. The SCSed products were also further calcined at 500 and 700 ºC for 2 h in air for comparison.

The glycine-nitrate combustion synthesis of KNN can be given in the following equation: [24, 31]

$$0.5\ KNO_3 + 0.5\ NaNO_3 + 0.5\ Nb_2O_5 + n\ C_2H_5O_2N + (4.5n\text{-}2.5)\ O_2 \rightarrow K_{0.5}Na_{0.5}NbO_3 + 2n\ CO_2 + 2.5n\ H_2O + (0.5 + 0.5n)\ N_2 \quad (1)$$

The nature of the combustion behavior is governed by the oxidizing/reducing characteristics of the nitrate-glycine, which can be quantified using the combustion equivalence ratio, ϕ. Here, ϕ is determined by the ratio between the total valencies of fuels and the total valencies of nitrate oxidizers: [31]

$$\phi = \frac{total\ valencies\ of\ glycine}{total\ valencies\ of\ nitrates} = \frac{9n}{5} \quad (2)$$

Here, it is assumed that CO_2, N_2, and H_2O were the only gaseous combustion emissions since they are the most stable gases products. The valencies of the elements are assumed to be C (+4), H (+1), N (0), O (-2), Na (+1) and K (+1), respectively. Here, ϕ = 1 indicates a

stoichiometric combustion condition, $\phi < 1$ indicates an insufficient fuel condition, whereas $\phi > 1$ means an excess fuel condition. In this study, seven samples at ϕ = 0.6, 0.8, 1.0, 1.2, 1.4, 1.6 and 1.8 were prepared, with the corresponding *n* value of 1/3, 4/9, 5/9, 2/3, 7/9, 8/9, and 1, respectively.

For the scaling-up production of KNN, one batch of 100 g was also prepared in the same manner by using electric mantle heater. As a comparison, the dried gel raw materials were also heated by a microwave oven for the one-step SCS of KNN.

Material characterization: Scanning electron microscopy (SEM, JEOL, JSM-7400F) was used for observing the morphology and particle size of the samples. Powder X-ray diffraction (XRD, Rigaku Miniflex, Cu-Kα) was used to characterize the phase compositions of the obtained materials. The stability of the one-step SCSed products were studied using a thermogravimetric (TG) analyzer (Mettler Toledo), in which the samples were subjected to a heating rate of 10 ^{o}C min^{-1} in air flow.

3. Results and discussion

Figure 2 shows the typical temperature histories during SCS at different ϕ values, which were measured by inserting a K-type thermocouple in the reactants. It is noted that temperature jumping increase are observed at around 300 ºC for all samples, excluding at ϕ = 0.6. The steep temperature jumps indicate the occurrence of the typical self-sustaining SCS. At ϕ = 1.0, the measured temperature presents the highest maximum value, indicating the sufficient and most intensive combustion reaction at the stoichiometric condition. However, at ϕ = 0.6, due to the insufficient feeding of glycine fuel, the typical temperature jump is not observed, inducing a non-self-sustaining combustion reaction.

Figure 3 presents the pictures of the products in the crucibles after the single step SCS at a 3 g-scale. It is noted that all samples, excluding at ϕ = 0.6, present white powdery products in the crucible. Sample at ϕ = 1.0 presents the whitest color, which is a clue of high-purity product under sufficient combustion.

The one-step combusted samples were characterized by XRD for their phase compositions, as shown in Figure 4. It is noted that excluding the sample at ϕ = 0.6, all samples present a single phase of KNN (JCPDS no. 33‑1270) even that the combustion reaction time is very short (~several minutes). At ϕ = 0.6, the sample is not well sintered to form KNN since that the high-temperature SCS reaction does not proceed well at this insufficient fuel condition. The crystallite size, *t*, of the SCSed samples was calculated using the Scherer’s equation:

$$t = \frac{K\lambda}{B\ cos\theta} \qquad (3)$$

here K is the shape factor (K = 1.0 was used in study), λ is the X-ray wavelength, B is the line broadening (measured in radians) at half the maximum intensity, and θ is the Bragg angle. The strongest peaks at 2θ = 3.18º was used for the calculation. The calculated crystallite sizes are 18.6, 22.5, 20.2, 18.3, 17.1 and 15.2 nm for the samples from ϕ = 0.8 to ϕ = 1.8, respectively. Sample obtained at ϕ = 1.0 represent the largest crystallite size, which is due to most sufficient combustion at stoichiometric fuel condition with the highest combustion flame temperature. With the increase of fuel amount, the crystallite size of the SCSed samples decreases which can be ascribed to the decrease of combustion flame temperature at fuel-excess condition and more gas emission that can avoid the great sintering the combusted powdery product as well.

To further evaluate the effect of sintering temperature on the formation of KNN, the SCSed samples were subsequently calcined at 500 and 700 ºC, respectively. As indicative by XRD phase composition measurement in Figures 5 and 6, sample at ϕ = 0.6 is the only one which shows the phase composition change upon sintering. After sintering at 500 ºC for 2 h for sample at ϕ = 0.6, a pure KNN phase is still not formed, however, when the sintering temperature is increased to 700 ºC, a single phase of KNN is observed. This result indicates that

for the formation of KNN by sintering, a high temperature of larger than 700 ºC is needed. Moreover, by adjusting the glycine-nitrate ratio, it is possible to achieve a high combustion temperature that is enough for the fast sintering to produce KNN in a single-step of short-time SCS.

To further evaluate the stability of the one-step SCSed KNN, the samples were subjected to TG analysis under air flow, which were heated to 1000 ºC at a temperature ramp of 10 ºC min^{-1}. Figure 7 shows the TG curves. It is observed that for the samples obtained at or slightly higher than the stoichiometric condition, including ϕ = 1.0, 1.2 and 1.4, the TG curves present a small weight decrease at around 600 ºC. The TG curve for the sample obtained at ϕ = 1.6 present gradually weight decrease starting from around 200 ºC, which represents the combustion of carbonaceous residues due to the addition of excess amount of glycine fuel. However, for the sample obtained at the fuel-insufficient condition (ϕ = 0.8), the TG curve represents an obvious weight decrease at around 600 ºC, which is due to the insufficient formation of KNN. The weight change for sample ϕ = 0.6 is even severer. Therefore, it is concluded that the stoichiometric or slightly fuel-excess condition is good for the one-step SCS of KNN.

The above results are based on the synthesis of a 3 g-scale. To further evaluate the scaling-up productivity of the one-step SCS for KNN, the experiments were also conducted at a 100 g-scale under the stoichiometric condition. The SCS reactions were initiated by both

electric heating and microwave heating. It is observed from the XRD patterns in Figure 8-(a), both samples show the single phase of KNN. The real image of the self-sustaining combustion reaction is shown in Figure 8-(b), while the final product at a 100 g-scale is shown in Figure 8-(c).

Figure 9 shows the SEM images of one-step SCSed KNN obtained at different fuel conditions. All samples, excluding the one at ϕ = 0.6, show the agglomerate of cubic nanoparticles. Sample obtained at ϕ = 0.6 shows large bulky agglomerates as the secondary particles in the range of several hundreds of microns; the bulky agglomerate for this sample is also difficult to be de-agglomerated. At a large magnification observation from SEM, this sample presents primary particles with irregular shapes, which are greatly melted together due to their nitrate precursors. With the increasing amount of added glycine to obtain a sufficient combustion reaction (with ϕ > 0.8), the observed primary particles show many cubic nanoparticles, which are the well-crystallined KNN with size ranging from around 100 nm to several hundreds of nanometers. Although the secondary particles of the samples at ϕ > 0.8 still present many large agglomerates with size up to dozens of microns, these samples are very easy to be pulverized and de-agglomerated. With the increasing amount of added glycine, the powders of the samples become easier to be re-dispersed. This is because of that with the increasing amount of added glycine, larger amount of gases emitted during combustion reaction,

which can avoid the great sintering of the samples at high-temperature flame.

4. Conclusions

Powdery products of KNN have been manufactured by a single step SCS, which is a self-sustaining exothermic process. Specifically, glycine was used as the reductant fuel, while potassium and sodium nitrates were used as the oxidizers, which were mixed with niobium oxide powders. By adjusting the added glycine amount, KNN product of a single phase could be successfully prepared in a one-step SCS. It is also concluded that the stoichiometric or slightly fuel-excess condition was good for the single step production of KNN. The one-step SCS production of KNN was also scalable, which can be ignited by both electric heating and microwave heating. This work offers a successful example of the one-step production of KNN by a feasible and scalable SCS process, which can be extended to the production of various functional ceramic oxides.

References

[1] N. Fumio, F. Marina, A Review on Piezoelectric, Magnetostrictive, and Magnetoelectric Materials and Device Technologies for Energy Harvesting Applications, Advanced Engineering Materials, 20 (2018)

1700743.
[2] S.W. M., B.N. S., B. Lennart, Novel Powder‐Processing Methods for Advanced Ceramics, Journal of the American Ceramic Society, 83 (2000) 1557-1574.
[3] X. Wang, J. Wu, D. Xiao, J. Zhu, X. Cheng, T. Zheng, B. Zhang, X. Lou, X. Wang, Giant Piezoelectricity in Potassium–Sodium Niobate Lead-Free Ceramics, Journal of the American Chemical Society, 136 (2014) 2905-2910.
[4] J. Wu, D. Xiao, J. Zhu, Potassium–Sodium Niobate Lead-Free Piezoelectric Materials: Past, Present, and Future of Phase Boundaries, Chemical Reviews, 115 (2015) 2559-2595.
[5] J. Wu, D. Xiao, J. Zhu, Potassium–sodium niobate lead-free piezoelectric ceramics: recent advances and perspectives, Journal of Materials Science: Materials in Electronics, 26 (2015) 9297-9308.
[6] X.-Q. Fang, J.-X. Liu, V. Gupta, Fundamental formulations and recent achievements in piezoelectric nano-structures: a review, Nanoscale, 5 (2013) 1716-1726.
[7] S. Lanfredi, L. Dessemond, A.C. Martins Rodrigues, Dense ceramics of NaNbO3 produced from powders prepared by a new chemical route, Journal of the European Ceramic Society, 20 (2000) 983-990.
[8] W. Liu, Dielectric and sintering properties of NaNbO3 ceramic prepared by Pechini method, J Electroceram, 31 (2013) 376-381.
[9] J. Heng, S.T. Ting, G. Hong, Z.Y. Chun, Direct preparation of K0.5Na0.5NbO3 powders, Crystal Research and Technology, 46 (2011) 85-89.
[10] L. Nan, W. Ke, L. Jing‐Feng, L. Zonghuai, Hydrothermal Synthesis and Spark Plasma Sintering of (K, Na)NbO3 Lead‐Free Piezoceramics, Journal of the American Ceramic Society, 92 (2009) 1884-1887.
[11] K.-i. Kakimoto, Y. Hayakawa, I. Kagomiya, Low-Temperature Sintering of Dense (Na,K)NbO3 Piezoelectric Ceramics Using the Citrate Precursor Technique, Journal of the American Ceramic Society, 93 (2010) 2423-2426.
[12] C. Wattanawikkam, N. Vittayakorn, T. Bongkarn, Low temperature fabrication of lead-free KNN-LS-BS ceramics via the combustion method, Ceramics International, 39 (2013) S399-S403.
[13] H. Yang, Y. Lin, J. Zhu, F. Wang, An efficient approach for direct synthesis of K0.5Na0.5NbO3 powders, Powder Technology, 196 (2009) 233-236.
[14] N. Chaiyo, R. Muanghlua, Y. Wongprasert, P. Seeharaj, N. Vittayakorn, Combustion Synthesis of Lead-free Piezoelectric Alkali Metal Niobate Family, Ferroelectrics, 453 (2013) 26-37.
[15] S.T. Aruna, A.S. Mukasyan, Combustion synthesis and nanomaterials, Current Opinion in Solid State and Materials Science, 12 (2008) 44-50.
[16] A. Varma, A.S. Mukasyan, A.S. Rogachev, K.V. Manukyan, Solution Combustion Synthesis of Nanoscale Materials, Chemical Reviews, (2016).
[17] F.-t. Li, J. Ran, M. Jaroniec, S.Z. Qiao, Solution combustion synthesis of metal oxide nanomaterials for energy storage and conversion, Nanoscale, 7 (2015) 17590-17610.

[18] W. Wen, J.-M. Wu, Nanomaterials via solution combustion synthesis: a step nearer to controllability, RSC Advances, 4 (2014) 58090-58100.
[19] Y. Liu, M. Qin, L. Zhang, M. Huang, S. Li, B. Jia, D. Zhang, X. Qu, Solution combustion synthesis of nanocrystalline Fe–50%Ni alloy powder, Powder Technology, 267 (2014) 68-73.
[20] A. Ashok, A. Kumar, R.R. Bhosale, M.A.H. Saleh, U.K. Ghosh, M. Al-Marri, F.A. Almomani, M.M. Khader, F. Tarlochan, Cobalt oxide nanopowder synthesis using cellulose assisted combustion technique, Ceramics International, 42 (2016) 12771-12777.
[21] G.K. Pradhan, S. Martha, K.M. Parida, Synthesis of Multifunctional Nanostructured Zinc–Iron Mixed Oxide Photocatalyst by a Simple Solution-Combustion Technique, ACS Applied Materials & Interfaces, (2011).
[22] K. Deshpande, A. Mukasyan, A. Varma, Direct Synthesis of Iron Oxide Nanopowders by the Combustion Approach: Reaction Mechanism and Properties, Chemistry of Materials, 16 (2004) 4896-4904.
[23] C. Zhu, A. Nobuta, G. Saito, I. Nakatsugawa, T. Akiyama, Solution combustion synthesis of LiMn2O4 fine powders for lithium ion batteries, Advanced Powder Technology, 25 (2014) 342-347.
[24] C. Zhu, A. Nobuta, I. Nakatsugawa, T. Akiyama, Solution combustion synthesis of LaMO3 (M = Fe, Co, Mn) perovskite nanoparticles and the measurement of their electrocatalytic properties for air cathode, International Journal of Hydrogen Energy, 38 (2013) 13238-13248.
[25] C.-G. Han, C. Zhu, N. Sheng, Y. Aoki, H. Habazaki, T. Akiyama, A facile one-pot synthesis of FeOx/carbon/graphene composites as superior anode materials for lithium-ion batteries, Electrochimica Acta, 235 (2017) 88-97.
[26] D.P. Tarragó, C.d.F. Malfatti, V.C. de Sousa, Influence of fuel on morphology of LSM powders obtained by solution combustion synthesis, Powder Technology, 269 (2015) 481-487.
[27] X. Wang, M. Qin, F. Fang, B. Jia, H. Wu, X. Qu, A.A. Volinsky, Solution combustion synthesis of nanostructured iron oxides with controllable morphology, composition and electrochemical performance, Ceramics International, 44 (2018) 4237-4247.
[28] P. Palei, M. Pattanaik, P. Kumar, Effect of oxygen sintering on the structural and electrical properties of KNN ceramics, Ceramics International, 38 (2012) 851-854.
[29] C.-G. Han, C. Zhu, G. Saito, T. Akiyama, Glycine/sucrose-based solution combustion synthesis of high-purity LiMn2O4 with improved yield as cathode materials for lithium-ion batteries, Advanced Powder Technology, 26 (2015) 665-671.
[30] C. Zhu, A. Nobuta, Y.-W. Ju, T. Ishihara, T. Akiyama, Solution combustion synthesis of Ce0.6Mn0.3Fe0.1O2 for anode of SOFC using LaGaO3-based oxide electrolyte, International Journal of Hydrogen Energy, 38 (2013) 13419-13426.
[31] S.R. Jain, K.C. Adiga, V.R. Pai Verneker, A new approach to thermochemical calculations of condensed fuel-oxidizer mixtures, Combustion and Flame, 40 (1981) 71-79.

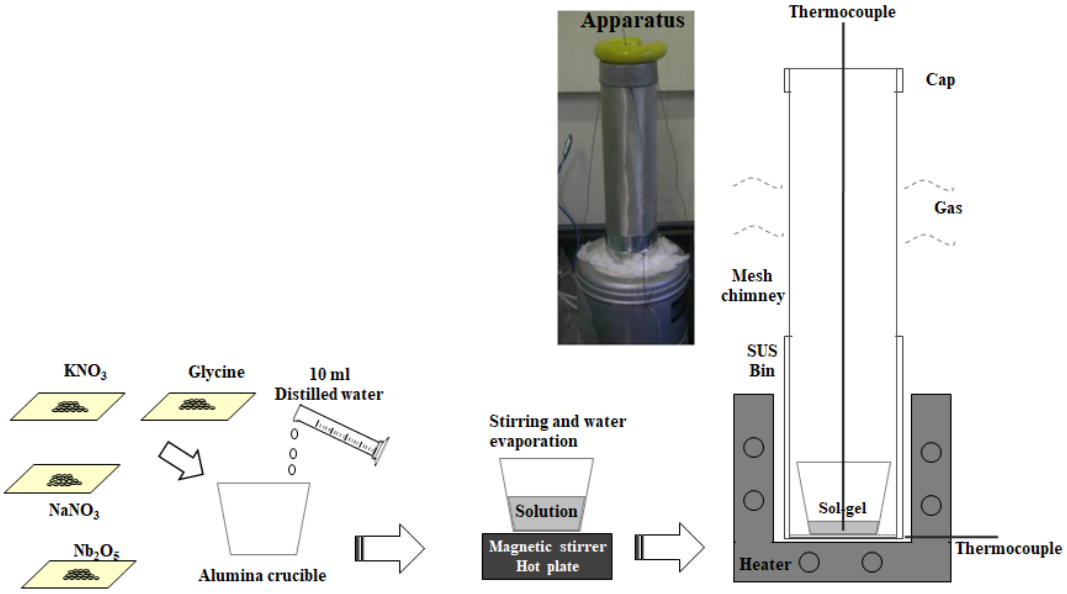

Figure 1. Schematic diagram of the experimental setup.

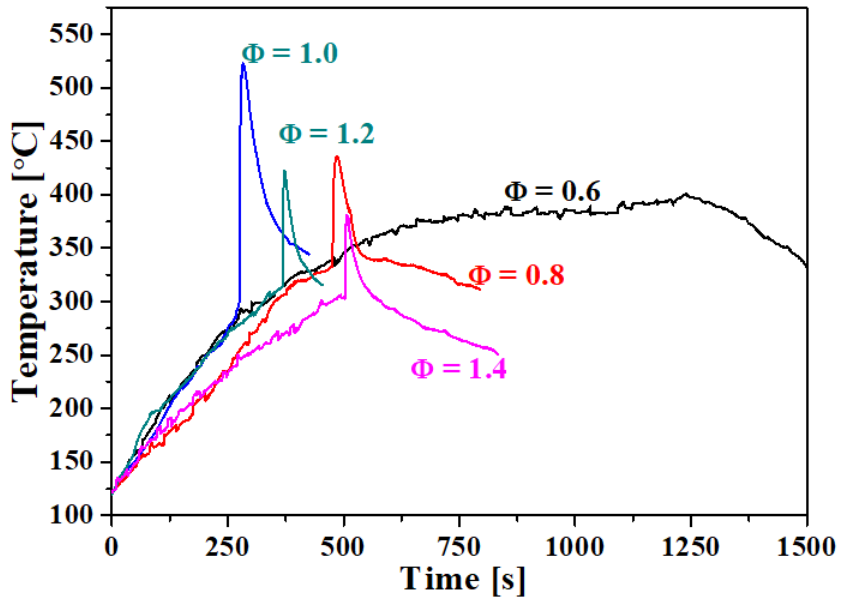

Figure 2. Temperature history during SCS at different Φ values, which is measured by inserting a K-type thermocouple in the reactants.

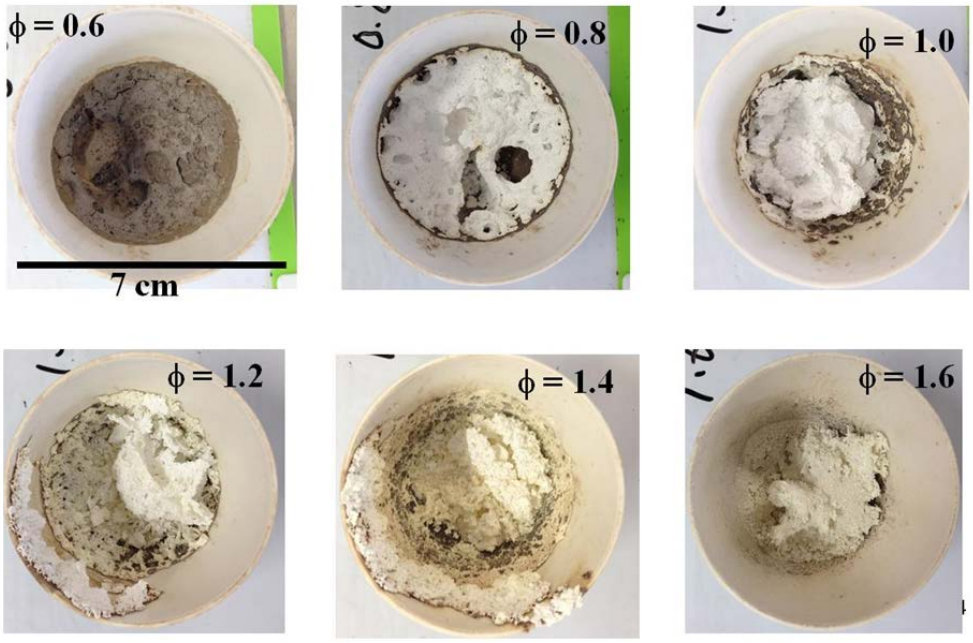

Figure 3. Pictures of the products after the one-step SCS at the 3 g-scale.

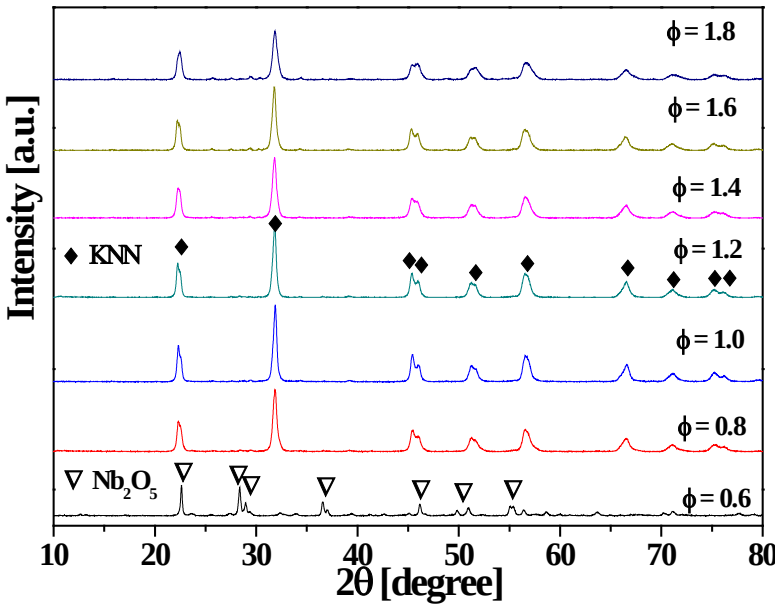

Figure 4. XRD patterns of the samples after one-step SCS.

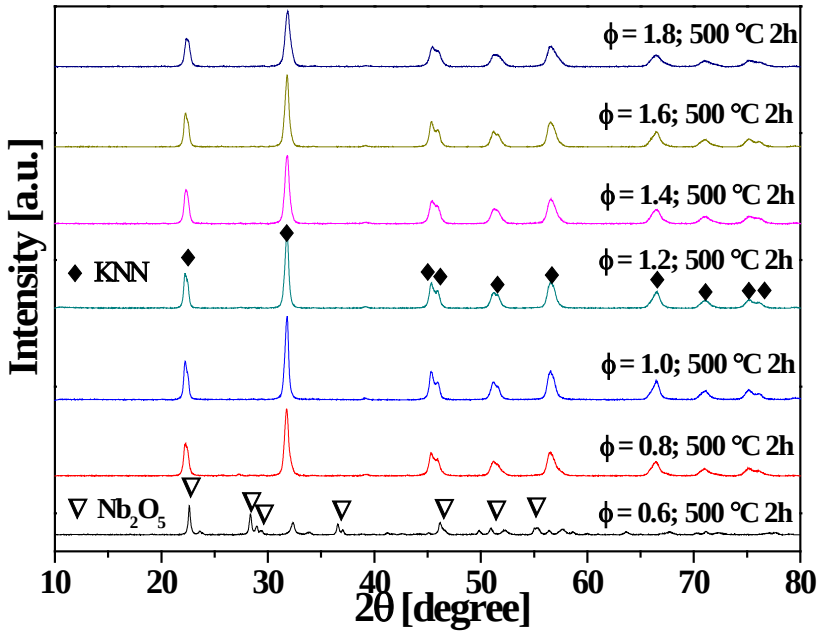

Figure 5. XRD patterns of the samples after SCS then calcined at 500 ºC for 2 h.

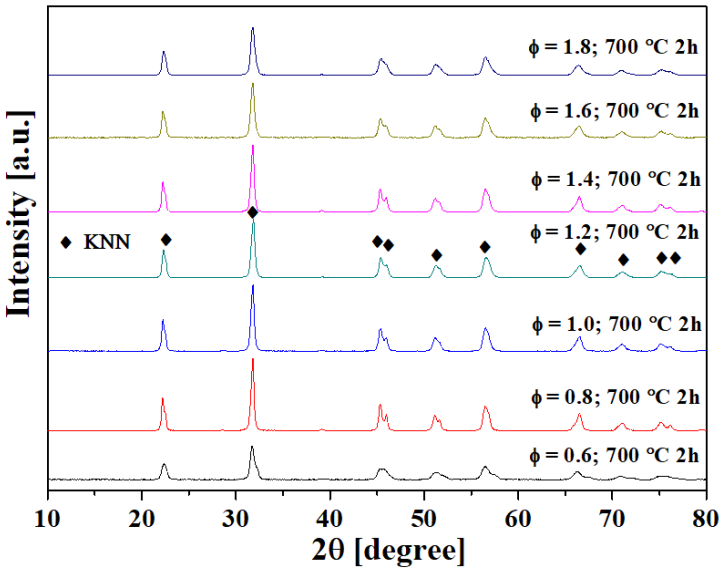

Figure 6. XRD patterns of the samples after SCS then calcined at 700 ºC for 2 h.

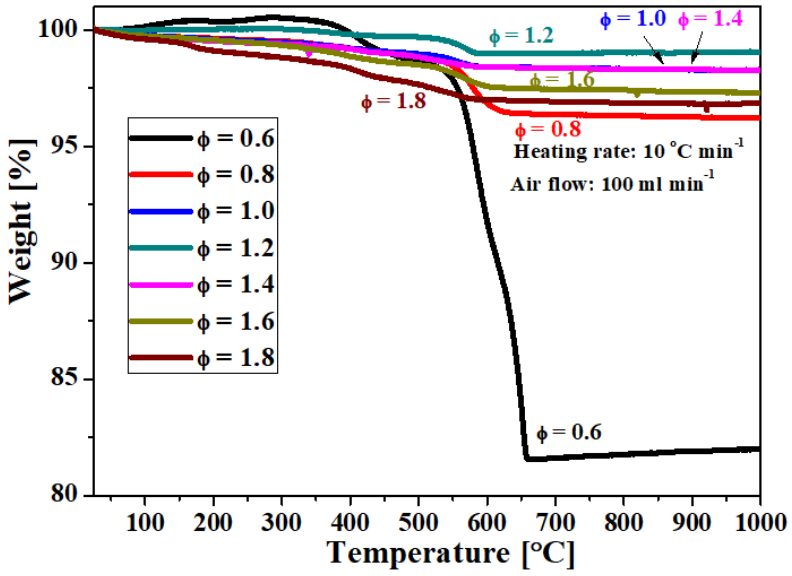

Figure 7. TG analysis of the SCSed samples under air flow.

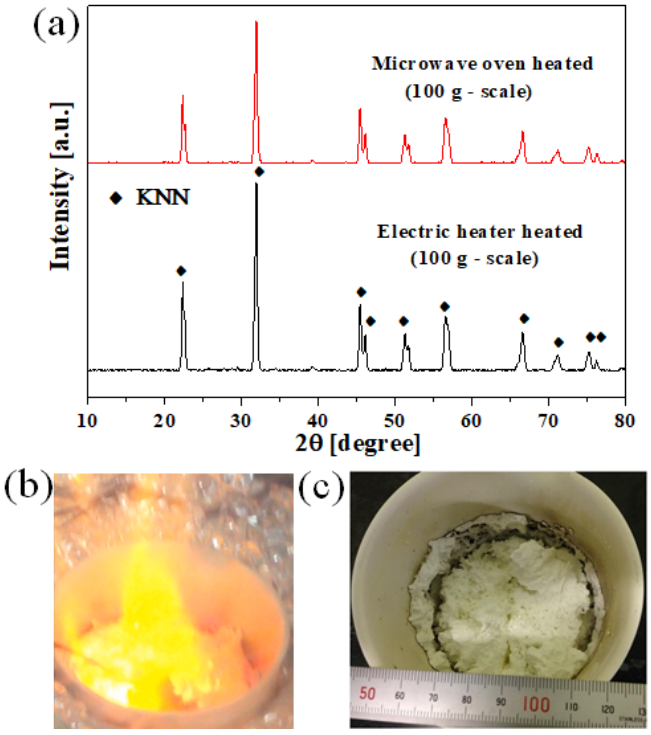

Figure 8. Analysis of the KNN products after one-step SCS at a 100 g scale, which were synthesized by microwave and electric heating. (a) XRD patterns; (b) the image of reaction during combustion in a 300 mL crucible; (c) the product image in the crucible.

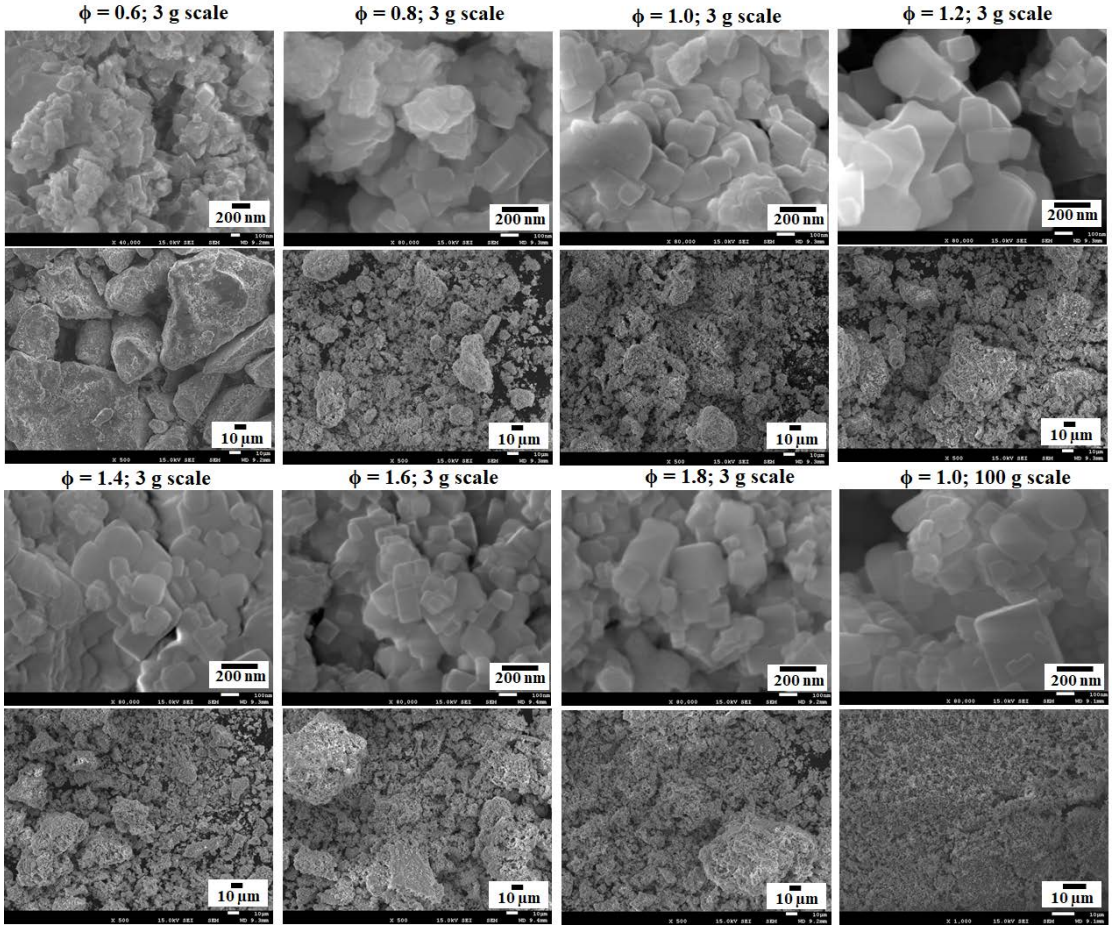

Figure 9. SEM images of the products after one-step SCS.